Onset of fluidization in vertically shaken granular material

Thorsten Pöschel,[1,2] Thomas Schwager,[2] and Clara Salueña[2]

[1]*ICA 1, Universität Stuttgart, Pfaffenwaldring 27, D-70569 Stuttgart, Germany*
[2]*Institut für Physik, Humboldt-Universität zu Berlin, Invalidenstraße 110, D-10115 Berlin, Germany*

When granular material is shaken vertically one observes convection, surface fluidization, spontaneous heap formation, and other effects. There is a controversial discussion in the literature as to whether there exists a threshold for the Froude number $\Gamma = A_0 \omega_0^2/g$, below which these effects cannot be observed anymore. By means of theoretical analysis and computer simulation we find that there is no such single threshold. Instead, we propose a modified criterion that coincides with the critical Froude number $\Gamma_c = 1$ for small driving frequency ω_0.

PACS number(s): 45.05.+x, 46.40.−f, 81.05.Rm, 83.70.Fn

I. INTRODUCTION

When granular material in a rectangular container is exposed to vertical oscillations under certain conditions one observes a variety of effects, such as convection [1–3], surface fluidization [4–8], spontaneous heap formation [9,10], surface patterns [11,12], oscillons [13], and others. The common feature of all these effects is that particles change their position with respect to each other. Provided the particles do not change their mechanical properties during the observation time (by polishing, comminution, etc.) the condition for this motion is that neighboring particles separate from each other at least for a small part of the oscillation cycle $T = 2\pi/\omega_0$.

There is a controversial discussion in the literature as to whether there is a critical value of the Froude number

$$\Gamma_c = A_0 \omega_0^2/g, \tag{1}$$

below which the above mentioned effects vanish, with A_0 and ω_0 being the parameters of the sinusoidal motion of the container. In *many* experimental observations (e.g., [1,6,7,10,11,14,15]) and computer simulations (e.g., [15,16]) such a critical number Γ_c was found. Several authors believe that the value is $\Gamma_c = 1$. In numerical simulations, however, surface fluidization and convection have been found for $\Gamma \lesssim 1$ [3,8,17]. Therefore, some authors believe that Γ is not the proper criterion to determine the degree of fluidization of a granular system [5,18].

In this article we discuss the response of granular material to vertical oscillation in the limit of a one dimensional approach: the lowest bead of a vertical column of N identical spherical beads is shaken with periodicity $z_0 = A_0 \cos \omega_0 t$ and the other beads move due to their interaction force and gravity g. We study the motion of the entire column and can show that particles can lose contact with their neighbors even when $\Gamma = A_0 \omega_0^2/g$ is significantly less than 1.

Adjacent spheres k and $k+1$ of radius r and mass m at vertical positions z_k and z_{k+1} interact with their next neighbors by

$$F_{k,k+1} = -\sqrt{r}(\mu \xi_{k,k+1}^{3/2} + \alpha \dot{\xi}_{k,k+1} \sqrt{\xi_{k,k+1}}) \tag{2}$$

with

$$\mu = \frac{\sqrt{2}}{3} \frac{Y}{1-\nu^2},$$

$$\alpha = \frac{\sqrt{2}}{3} \frac{YA}{1-\nu^2}$$

being the elastic and dissipative material constants, i.e., functions of the Young modulus Y, Poisson ratio ν, and dissipation rate A [for details of the derivation of Eq. (2) see [19]]. ξ is the compression $2r - |z_k - z_{k+1}|$ of the spheres. The height of the column is $L = 2Nr$. Expression (2) is valid if the typical relative velocities of adjacent spheres are far below the speed of sound in the material of the spheres. Certainly this condition holds for typical vibration experiments.

Introducing new coordinates $u_k = z_k - 2rk$ $(k = 0, \ldots, N)$, the compression of two adjacent spheres is

$$\xi_{k,k+1} = u_k - u_{k+1}. \tag{3}$$

Applying these definitions in Eq. (2) and adding gravity g we get

$$\ddot{z}_k = \frac{1}{m}(F_{k,k+1} - F_{k-1,k}) - g, \tag{4}$$

$$F_{k,k+1} = -\mu\sqrt{r}(u_k - u_{k+1})^{3/2} - \alpha\sqrt{r}(\dot{u}_k - \dot{u}_{k+1})\sqrt{u_k - u_{k+1}}.$$

The 0th sphere is fixed at the oscillating table; hence its position is

$$z_0(t) = u_0(t) = A_0 \cos \omega_0 t.$$

We are interested in the critical parameters of driving (A_0, ω_0) when the Nth particle loses contact, i.e., when $u_N > u_{N-1}$. We define the ''response'' $R(\omega_0)$ as the ratio A_N/A_0 where A_N is the amplitude of the Nth particle at frequency ω_0 and A_0 is the amplitude of the driving vibration. $R(\omega_0)$ can be calculated by convoluting the motion $z_N(t)$ with $\exp(i\omega_0 t)$. Supposing $A_N \omega_0^2/g \geq 1$, the Nth particle separates from the $(N-1)$st. If we found $A_0 < A_N$ the

critical Froude number $\Gamma_c = A_0 \omega_0^2 / g$ would be less than 1. We will show that there is a range of ω_0 where this is the case.

In the next section we will formulate the problem in a continuum approach and derive a nonlinear partial differential equation for the motion of the column of particles. This equation is solved in Sec. III in the limit of elastic material properties, i.e., by dropping the dissipative terms. Once the solution for the elastic case has been discussed in detail, it is easier to study the influence of the dissipative term and to derive the solution of the full equation of motion, which is done in Sec. IV. Section V compares the analytical results with a molecular dynamics simulation of the original (discrete) problem stated in Eq. (4). Finally, we discuss the results.

II. CONTINUUM APPROACH

To study the system analytically we use a one dimensional continuum approach. To this end we perform a Taylor expansion of the force with respect to the radius r and consequently consider the limit $r \to 0$, $N \to \infty$ with $2rN = L$ = const. First we have to replace the displacements u_k by $u(2kr)$, introducing the displacement field $u(z)$ which is a continuous function of z. With Eq. (3) we find from Taylor expansion

$$\xi_{k,k+1} = u(2kr) - u(2kr + 2r) = -2r(\partial u / \partial z)|_{z=2kr}.$$

The net force experienced by the kth particle is

$$\begin{aligned}
F_k = F_{k,k+1} - F_{k-1,k} &= -\mu \sqrt{r}(\xi_{k,k+1}^{3/2} - \xi_{k-1,k}^{3/2}) \\
&- \alpha \sqrt{r}(\dot{\xi}_{k,k+1}\sqrt{\xi_{k,k+1}} - \dot{\xi}_{k-1,k}\sqrt{\xi_{k-1,k}}) \\
&= -2\sqrt{2}r^2\mu \left[\left(-\frac{\partial u_k}{\partial z} \right)^{3/2} - \left(-\frac{\partial u_{k-1}}{\partial z} \right)^{3/2} \right] \\
&+ 2\sqrt{2}r^2\alpha \left[\frac{\partial^2 u_k}{\partial t \partial z} \sqrt{-\frac{\partial u_k}{\partial z}} - \frac{\partial^2 u_{k-1}}{\partial t \partial z} \sqrt{-\frac{\partial u_{k-1}}{\partial z}} \right],
\end{aligned}$$

with the abbreviations

$$u_k = u(2kr), \tag{5}$$

$$\frac{\partial u_k}{\partial z} = \frac{\partial u}{\partial z}\Big|_{z=2kr}. \tag{6}$$

Both expressions in square brackets are expanded again and Eq. (5) becomes

$$\frac{F_k}{m} = \frac{3\sqrt{2}}{\pi\rho} \left[-\mu \left(-\frac{\partial u}{\partial z} \right)^{3/2} + \alpha \frac{\partial^2 u}{\partial t \partial z} \sqrt{-\frac{\partial u}{\partial z}} \right].$$

With

$$\kappa = \frac{3\sqrt{2}\mu}{\pi\rho} = \frac{2Y}{\pi\rho(1-\nu^2)}, \tag{7}$$

$$\beta = \frac{3\sqrt{2}\alpha}{\pi\rho} = \frac{2YA}{\pi\rho(1-\nu^2)}, \tag{8}$$

the continuum formulation of Eq. (4) is

$$\frac{\partial^2 u}{\partial t^2} = -g - \frac{\partial}{\partial z} \left[\kappa \left(-\frac{\partial u}{\partial z} \right)^{3/2} - \beta \frac{\partial^2 u}{\partial t \partial z} \sqrt{-\frac{\partial u}{\partial z}} \right], \tag{9}$$

$$\frac{\partial u}{\partial z}\Big|_{z=L} = 0,$$

where g accounts for the gravitational force.

III. LIMIT OF ELASTIC PARTICLES

In the following we consider Eq. (9) in the limit of no damping ($\beta = 0$). Using new variables

$$x = 1 - \frac{z}{L}, \tag{10}$$

$$\tau = \left(\frac{g\kappa^2}{L^5} \right)^{1/6} t, \tag{11}$$

$$\Omega = \left(\frac{L^5}{g\kappa^2} \right)^{1/6} \omega, \tag{12}$$

$$\gamma = \left(\frac{g^2 L^5}{\kappa^2} \right)^{1/6}, \tag{13}$$

Eq. (9) becomes

$$\frac{\partial^2 u}{\partial \tau^2} = -\gamma^2 + \frac{1}{\gamma}\frac{\partial}{\partial x} \left[\left(\frac{\partial u}{\partial x} \right)^{3/2} \right], \tag{14}$$

$$\frac{\partial u}{\partial x}\Big|_{x=0} = 0. \tag{15}$$

Equation (14) is defined in the range $x \in [0,1]$. The time independent solution $U(x)$ of Eq. (14) is

$$U(x) = \frac{3}{5}\gamma^2 (x^{5/3} - 1). \tag{16}$$

The solution of Eq. (14) can be considered as a superposition of the static solution (16) and a perturbation $w(x,\tau)$. Inserting $u = U + w$ in Eq. (14) we find

$$\begin{aligned}
\frac{\partial^2 w}{\partial \tau^2} &= -\gamma^2 + \frac{1}{\gamma}\frac{\partial}{\partial x} \left(\frac{\partial U}{\partial x} + \frac{\partial w}{\partial x} \right)^{3/2} \\
&\approx -\gamma^2 + \frac{1}{\gamma}\frac{\partial}{\partial x} \left[\left(\frac{\partial U}{\partial x} \right)^{3/2} + \frac{3}{2}\sqrt{\frac{\partial U}{\partial x}}\frac{\partial w}{\partial x} \right] \\
&= \frac{3}{2}\frac{\partial}{\partial x} \left(x^{1/3}\frac{\partial w}{\partial x} \right). \tag{17}
\end{aligned}$$

By separation of variables $w = T(\tau, \Omega)X(x, \Omega)$, i.e., a standing wave ansatz, we obtain two ordinary differential equations for T and x:

$$\ddot{T} = -\Omega^2 T, \tag{18}$$

$$\frac{3}{2}\frac{d}{dx}\left(x^{1/3}\frac{dX}{dx}\right)=-\Omega^2 X, \qquad (19)$$

with Ω being a real number. For $T(\tau,\Omega)$ one gets

$$T\sim\exp(i\Omega\tau).$$

The solution of the spatial equation (19) can be found using the Ansatz

$$X(x,\Omega)=x^{1/3}f(y), \quad y=\frac{2}{5}\sqrt{6}\Omega x^{5/6},$$

which yields

$$y^2\frac{d^2 f}{dy^2}+y\frac{df}{dy}+\left(y^2-\frac{4}{25}\right)f=0. \qquad (20)$$

Equation (20) is the Bessel equation of order 2/5. Hence the solution of Eq. (19) is

$$X(x,\Omega)=\left(\frac{6}{25}\right)^{1/5}\Gamma\left(\frac{3}{5}\right)\Omega^{2/5}x^{1/3}J_{-2/5}\left(\frac{2}{5}\sqrt{6}\Omega x^{5/6}\right). \qquad (21)$$

An expression containing $J_{2/5}$ would be a solution too; however, it does not satisfy the condition (15). The prefactor in Eq. (21) has been chosen to assure $X(0,\Omega)=1$.

Hence the solution for a single vibrational mode u_Ω is

$$u_\Omega=\exp(i\Omega\tau)X(x,\Omega). \qquad (22)$$

Without prior knowledge the full solution of Eq. (17) has to be assumed to be a superposition of vibrational modes for all real (rescaled) frequencies Ω:

$$u=\int_{-\infty}^{\infty}d\Omega\,A(\Omega)\exp(i\Omega\tau)X(x,\Omega). \qquad (23)$$

In the steady state of pure sinusoidal excitation of the base, i.e., when all nonoscillatory perturbations that originate from the initialization have been damped out, Eq. (23) is the full (steady state) solution of Eq. (17).

The function $A(\Omega)$ represents the excitation of the mode at frequency Ω. The boundary condition at the top of the chain is automatically satisfied, whereas the boundary condition at the bottom reads

$$u(1,\tau)=\int_{-\infty}^{\infty}d\Omega\,A(\Omega)\exp(i\Omega\tau)X(1,\Omega) \qquad (24)$$

$$=A_0\cos\Omega_0\tau. \qquad (25)$$

One can see that the integrand of Eq. (24) can be nonzero only for $\Omega\neq\Omega_0$. This means that for $\Omega\neq\Omega_0$ either $A(\Omega)$ or $X(1,\Omega)$ has to be zero, i.e., for all frequencies for which $X(1,\Omega)$ is nonzero the amplitude must be zero, whereas for all frequencies that are a root of $X(1,\Omega)=0$ the amplitude can be nonzero. Therefore, we find that the full solution of Eq. (17) is a superposition of the vibrational mode of the frequency of shaking Ω_0 and of a discrete set of frequencies Ω_k $(k=1,\dots,\infty)$.
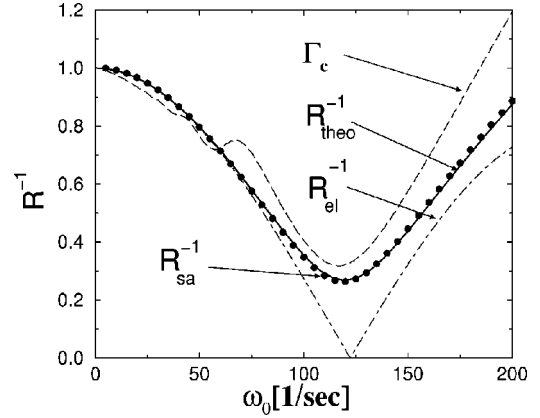

FIG. 1. The response function R_{el}^{-1} due to Eq. (26) for a column of elastic particles (dash-dotted). For dissipative particles ($\beta=127$ m^2/sec): circles, R_{sa}^{-1}, numerical integration of Eq. (4) at small amplitude; full line, R_{theo}^{-1}, analytical solution Eq. (36) of the full Eq. (9) including dissipation; dashed line, $\Gamma_c(\omega_0)$, result of a direct simulation of Eq. (4) (for explanation see text.)

Note that Ω_k are not rational multiples of each other since the roots of Bessel functions are incommensurable [see Eq. (21)]. Therefore, to determine the maximum acceleration of the topmost particle it is sufficient to consider only the mode of the external excitation. All other vibrational modes can only further increase the maximal acceleration.

The above defined response R is the ratio A_N/A_0. Since the zeroth particle corresponds to $x=1$ and the Nth to $x=0$, we can write

$$R^{-1}(\Omega_0)=\left|\frac{X(1,\Omega_0)}{X(0,\Omega_0)}\right|=|X(1,\Omega_0)|$$

$$=\left(\frac{6}{25}\right)^{1/5}\Gamma\left(\frac{3}{5}\right)\Omega_0^{2/5}\left|J_{-2/5}\left(\frac{2}{5}\sqrt{6}\Omega_0\right)\right|. \qquad (26)$$

The response R is an amplification factor; hence the value $g/R(\Omega_0)$ is the critical acceleration of the driving vibration [20]. R is larger than 1 for all driving frequencies ω_0. This means that for *any* driving frequency ω_0 and driving amplitude A_0 the amplitude of the top particle of the column A_N at frequency ω_0 will be larger than A_0. Therefore, for $A_N\omega_0^2/g=1$, i.e., when the Nth particle separates from the $(N-1)$st, we find $A_0\omega_0^2/g=\Gamma_c<1$.

According to the above arguments we have to replace the condition $\Gamma\geq1$, which was supposed to be the precondition for surface fluidization, convection, etc., by

$$A_0\omega_0^2/g=\Gamma\geq R^{-1}(\omega_0). \qquad (27)$$

The function $R^{-1}(\omega_0)$ vs ω_0 is drawn in Fig. 1 (dash-dotted line, R_{el}^{-1}). For the system parameters we used $A_0=0.01$ mm, elastic constant $\kappa=2.8\times10^4$ m^2/sec^2 (rubber with Young modulus $Y=4\times10^7$ Pa), and $L=0.6$ m. The curve reveals pronounced resonances at eigenfrequencies ω_k where R^{-1} becomes minimal (only the first resonance is shown in Fig. 1).

All experiments on surface fluidization and convection that can be found in the literature were performed far below

the first resonance, which for a 20 cm column of cast iron beads ($Y=10.8\times10^{10}$ N m^{-2}, $\rho=7.8\times10^{3}$ kg m^{-3}, $\nu=0.22$) is at about 330 Hz. This value can be found from the root of Eq. (26), i.e., $R^{-1}(\Omega_0)=0$, which yields $\Omega_0\approx1.78$, together with definitions (12) and (7). Therefore, of particular interest for practical purposes is the limit of small frequency ω_0, i.e., below the first eigenfrequency. The Taylor expansion of Eq. (26) yields $R^{-1}(\Omega_0)$ for small Ω_0,

$$R^{-1}=1-\frac{2}{5}\Omega_0^2+O(\Omega_0^4)$$

$$=1-\frac{2}{5}\left(\frac{L^5}{g\kappa^2}\right)^{1/3}\omega_0^2+O(\omega_0^4).$$

$$(28)$$

Given that the container vibrates with frequency ω_0, for the critical amplitude A_0 of the vibration when the top particle separates, i.e., when the material starts to fluidize, one finds

$$A_0=\frac{g}{\omega_0^2}-\frac{2}{5}\left(\frac{L^5}{g\kappa^2}\right)^{1/3}. \qquad (29)$$

Surprisingly, even for very small frequencies where $R^{-1}\rightarrow1$ one finds that the critical amplitude is reduced by a constant as compared with g/ω_0^2. So although the value of the response function comes arbitrarily close to 1, the critical *amplitude* differs from the expected one by a constant. However, this does not mean that the critical Froude number becomes a constant.

From the above equations (28) and (29) one can see that the size of the effect (the amplification) depends on $L^{5/3}$, $\rho^{2/3}$, and $Y^{-2/3}$, i.e., it increases with the length of the column and with the material density and decreases with increasing Y.

Equation (21) describes the behavior of a column of grains for the case of purely elastic contact ($\alpha=0$). If the dissipative material properties are taken into consideration the full equation (9), has to be solved which will be discussed in the following section.

IV. DISSIPATIVE PARTICLE INTERACTION

We will consider, as before, small perturbations w about the static deformation of the chain under gravity, which propagate from the bottom. The dissipative term is characterized by the parameter β in Eq. (9). From this equation, again introducing the static solution given by Eq. (16) and using the same transformation for the spatial coordinate $x\equiv1-z/L$, one obtains the corresponding linearized wave equation for dissipative materials,

$$\frac{\partial^2 w}{\partial t^2}=\left(\frac{g}{\kappa L^5}\right)^{1/3}\left[\frac{3}{2}\kappa\frac{\partial}{\partial x}\left(x^{1/3}\frac{\partial w}{\partial x}\right)+\beta\frac{\partial}{\partial x}\left(x^{1/3}\frac{\partial^2 w}{\partial t\partial x}\right)\right].$$

$$(30)$$

In this case it is less useful to introduce the rescaled time variable τ, while it proves convenient to define

$$\left(\frac{\kappa L^5}{g}\right)^{1/6}\equiv\ell, \qquad (31)$$

the natural length scale coming out of the analysis. By means of the Fourier transform

$$\mathcal{W}(x,\omega)=\frac{1}{\sqrt{2\pi}}\int_{-\infty}^{\infty}e^{-i\omega t}w(x,t)dt, \qquad (32)$$

Eq. (30) becomes

$$-\omega^2\mathcal{W}=\frac{\frac{3}{2}\kappa-i\omega\beta}{\ell^2}\frac{\partial}{\partial x}\left(x^{1/3}\frac{\partial\mathcal{W}}{\partial x}\right), \qquad (33)$$

which has the same structure as Eq. (19). Hence the same transformations apply in this case and the general solution reads finally

$$\mathcal{W}(x,\omega)=x^{1/3}\left[C_1 J_{2/5}\left(\frac{\frac{6}{5}\omega\ell}{\sqrt{\frac{3}{2}\kappa-i\omega\beta}}x^{5/6}\right)\right.$$
$$\left.+C_2 J_{-2/5}\left(\frac{\frac{6}{5}\omega\ell}{\sqrt{\frac{3}{2}\kappa-i\omega\beta}}x^{5/6}\right)\right]. \qquad (34)$$

The part of the solution depending on $J_{2/5}$ carries a divergence at $x=0$ ($z=L$), and therefore $C_1=0$ is required for the solution to be physical. The condition of the free end at $x=0$ ($z=L$) is satisfied automatically, as in the case $\beta=0$. The solution has exactly the same structure as the solution of the elastic problem, Eq. (21), and the only change is that the argument of the Bessel function has an imaginary part. If one considers only the mode ω_0, which propagates from the bottom ($x=1$) with amplitude A_0, the solution reads

$$w(x,t)=\text{Re}\left\{A_0 e^{i\omega_0 t}x^{1/3}\frac{J_{-2/5}\left(\frac{\frac{6}{5}\omega_0\ell}{\sqrt{\frac{3}{2}\kappa-i\omega_0\beta}}x^{5/6}\right)}{J_{-2/5}\left(\frac{\frac{6}{5}\omega_0\ell}{\sqrt{\frac{3}{2}\kappa-i\omega_0\beta}}\right)}\right\}.$$

$$(35)$$

The fluidization condition at the top of the chain $|\partial^2 w/\partial t^2(x=0,t)|>g$ can be written in general as

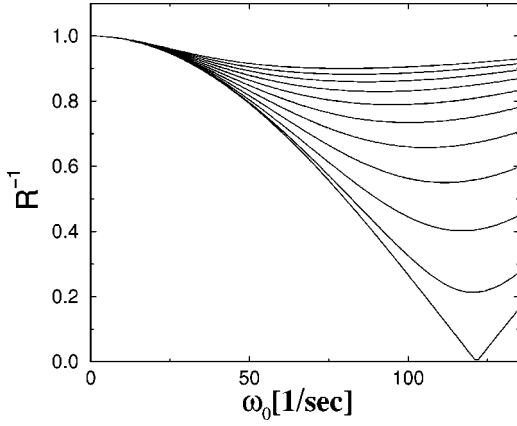FIG. 2. The response function over the frequency for different dissipative constants: $\beta = 0, 100, 200, \ldots, 1000$ m^2/sec (bottom to top). With increasing damping the minimum becomes less pronounced and shifts to lower frequencies.

$$R^{-1}(\omega_0) \equiv \Gamma\left(\frac{3}{5}\right) \left| \left(\frac{\frac{3}{5}\omega_0 \ell}{\sqrt{\frac{3}{2}\kappa - i\omega_0\beta}} \right)^{2/5} \right.$$

$$\left. \times J_{-2/5}\left(\frac{\frac{6}{5}\omega_0 \ell}{\sqrt{\frac{3}{2}\kappa - i\omega_0\beta}} \right) \right|$$

$$< \frac{A_0 \omega_0^2}{g}. \tag{36}$$

Since the Bessel functions of the first class have zeros only on the real axis, $R^{-1}(\omega_0)$ can no longer be zero for any frequency if $\beta \neq 0$. This means that the sharp resonances displayed by $R(\omega_0)$ when $\beta = 0$ disappear and are replaced by more or less pronounced minima in dependence on the damping constant β. This can also be observed in Fig. 1 (full line). Increasing values of β make the response smoother, it deviates from that of the elastic case earlier, and the local minima translate along the frequency axis appreciably (see Fig. 2).

Analogously to the elastic case [Eq. (28)], for small frequencies $R^{-1}(\omega_0)$ can be expanded into a Taylor series:

$$R^{-1} \simeq 1 - \omega_0^2 \frac{2}{5}\left(\frac{L^5}{g\kappa^2}\right)^{1/3} + \omega_0^4 \left(\frac{L^5}{g\kappa^2}\right)^{2/3}$$

$$\times \left[\frac{3}{100} + \frac{8}{45}\beta^2\left(\frac{g}{\kappa^4 L^5}\right)^{1/3} \right]. \tag{37}$$

The contribution due to the dissipative parameter enters the Taylor expansion at the fourth power of the frequency. Therefore, the analysis of the elastic case given by Eq. (28) remains valid for small frequencies.

It is interesting to note that due to Eq. (37) there *always* exists a global minimum below the value $R^{-1}(\omega_0) = 1$, regardless of the value of the dissipative parameter. We want to study for what range of frequencies the inverse response
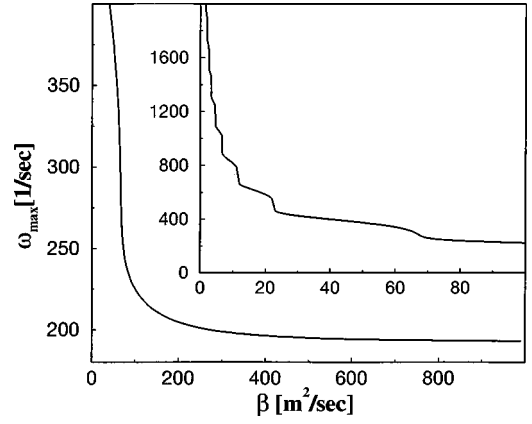

FIG. 3. The frequency ω_{max} at which the inverse response function becomes larger than 1 is almost constant with varying dissipative parameter β as long as the damping is not too small. For very low dissipative parameter β one finds a nonsmooth function (inset).

R^{-1} is smaller than 1 for varying damping constant β. The lower boundary of this interval is obviously $\omega = 0$. To determine the upper boundary ω_{max} we solved numerically the equation $R^{-1}(\omega_{max}) = 1$ for different values of β. The result of this calculation is shown in Fig. 3.

One can see that for high enough damping this frequency ω_{max} varies only slowly with β. The curve almost saturates at $\omega_{max} \approx 200$ sec^{-1} which is close to the first maximum of the undamped inverse response (see Fig. 4, dash-dotted line). Although the valley of the inverse response function becomes smaller with increasing damping (Fig. 3), even for larger damping R^{-1} is smaller than 1 in a finite frequency interval, i.e., the effect of amplitude amplification exists for almost the entire range of frequencies between zero and the first maximum of the undamped inverse response.

For small enough damping the frequency range of amplitude amplification $R^{-1}(\omega_0) < 1$ extends beyond the position of the first maximum of the undamped inverse response. Figure 4 shows the response function for different values of the dissipative parameter β together with the elastic case ($\beta = 0$, dash-dotted). The frequency ω_0 at which $R^{-1}(\beta) = 1$
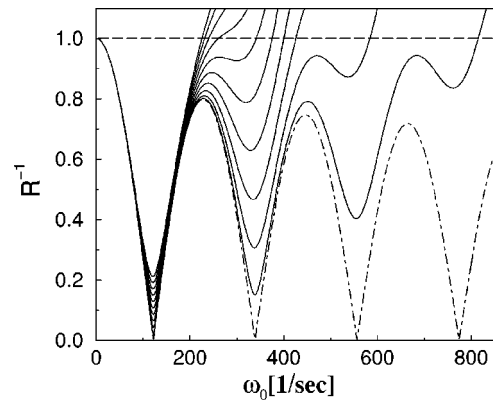

FIG. 4. The response function for different values of the dissipative constant $\beta = 10, 20, 30, \ldots, 100$ m^2/sec (bottom to top) together with the elastic curve $\beta = 0$ (dash-dotted). With decreasing β the curves are influenced by higher order minima of the response function. This explains the steps in the curve drawn in Fig. 3 for small values of the dissipation β.

increases with decreasing damping. In Fig. 4 one can clearly see the widening of the range of amplitude amplification. If we decrease the damping parameter, starting at high values where the amplifying range is limited to the first ''well,'' we cannot expect a large change since, as long as we remain limited to the first well, there is an upper bound (the frequency of the first maximum of R^{-1}) to this range. Reducing β further we will eventually reach values for which the amplifying range extends to the second well. Even for values of β that are only slightly below this threshold, the range will now span again almost the entire range of the second well up to the frequency of the second maximum. So there will be rather sharp steps in the dependence of the upper range limit of the damping instead of only gradual changes. This behavior explains the steps in the inset of Fig. 3.

V. NUMERICAL RESULTS

To check the analytical results and in particular the validity of the continuum approach, we calculated R^{-1} for a finite value of damping β from the numerical simulation of Eq. (4). The circles in Fig. 1 display the reciprocal response R^{-1} vs ω_0 with fixed amplitude $A_0 = 0.01$ mm, elastic constant $\kappa = 2.8 \times 10^4$ m^2/sec^2 (rubber with Young modulus $Y = 4 \times 10^7$ Pa), and $L = 0.6$ m. Figure 1 shows that for small frequency ω_0 and small damping α the undamped theoretical curve (dash-dotted) agrees well with numerical data. If one compares the numerical result with the damped solution according to Eq. (36) (full line in Fig. 1) the agreement with theory is very good.

To check the validity of our linear theory we also determined directly by integrating Eq. (4) at what Froude number Γ_c the particles start to jump. The results of this calculation are shown in the dashed curve in Fig. 1 and agree well with the linear theory. To obtain the value of Γ_c for a given frequency ω_0, we determined an upper bound A_0^+ for the critical amplitude where one observes jumping and a lower bound A_0^- where no jumping occurs. Then we narrowed the interval $A_0^+ - A_0^-$ by testing an amplitude between A_0^+ and A_0^- until $(A_0^+ - A_0^-)/A_0^+ < 10^{-3}$.

VI. DISCUSSION

For the case of a vertical column of viscoelastic spheres we derived a linear wave equation in a one dimensional approximation. We have shown that the sphere on top of the column, N, can separate from the $(N-1)$st even if the container is oscillated with $A_0 \omega_0^2/g < 1$. As the main result we derived a modified condition for the topmost particle to separate from its neighbor. We showed that instead of the widely accepted condition $\Gamma_c \equiv A_0 \omega_0^2/g > 1$ one has to satisfy $A_0 \omega_0^2/g > R^{-1}$, where R^{-1} is a function of ω_0. We have shown that independent of the material properties there *always* exists a range $\omega_0 \in [0, \omega_{max}]$ for which the amplitude of vibration A_0 is amplified, i.e., for which the top particle can separate (the material fluidizes) even if $A_0 \omega_0^2/g < 1$. Numerical calculations agree well with the analytical results.

Whereas the critical Froude number $\Gamma_c \geq 1$ is certainly the proper criterion to predict whether a single rigid particle will jump on a vibrating table, we suspect that this number is not suited to describe the behavior of a vibrated column of spheres, and even less is it a criterion for surface fluidization of a three dimensional granular material.

[1] E.E. Ehrichs, H.M. Jaeger, G.S. Karczmar, J.B. Knight, V.Yu. Kuperman, and S.R. Nagel, Science **267**, 1632 (1995); J.B. Knight, E.E. Ehrichs, V.Yu. Kuperman, J.K. Flint, H.M. Jaeger, and S.R. Nagel, Phys. Rev. E **54**, 5726 (1996); J.B. Knight, H.M. Jaeger, and S.R. Nagel, Phys. Rev. Lett. **70**, 3728 (1993); J.A.C. Gallas, H.J. Herrmann, T. Pöschel, and S. Sokolowski, J. Stat. Phys. **82**, 443 (1996); J. Duran, T. Mazozi, E. Clément, and J. Rajchenbach, Phys. Rev. E **50**, 5138 (1994).

[2] J.A.C. Gallas, H.J. Herrmann, and S. Sokolowski, Phys. Rev. Lett. **69**, 1371 (1992).

[3] Y-h. Taguchi, Phys. Rev. Lett. **69**, 1367 (1992); Europhys. Lett. **24**, 203 (1993).

[4] S. Warr, J.M. Huntley, and G.T.H. Jacques, Phys. Rev. E **52**, 5583 (1995).

[5] J.A.C. Gallas, H.J. Herrmann, and S. Sokolowski, Physica A **189**, 437 (1992).

[6] Y-h. Taguchi, J. Phys. II **2**, 2103 (1992); P. Evesque, E. Szmatula, and J.P. Denis, Europhys. Lett. **12**, 623 (1990).

[7] E. Clément, S. Luding, A. Blumen, J. Rajchenbach, and J. Duran, Int. J. Impact Eng. **7**, 1807 (1993).

[8] S. Luding, H.J. Herrmann, and A. Blumen, Phys. Rev. E **50**, 3100 (1994).

[9] M. Faraday, Philos. Trans. R. Soc. London **121**, 299 (1831); F. Dinkelacker, A. Hübler, and E. Lüscher, Biol. Cybern. **56**, 51 (1987); J. Rajchenbach, Europhys. Lett. **16**, 149 (1991).

[10] S. Douady, S. Fauve, and C. Laroche, Europhys. Lett. **8**, 621 (1989); H.K. Pak and R.P. Behringer, Nature (London) **371**, 231 (1994).

[11] F. Melo, P. Umbanhowar, and H.L. Swinney, Phys. Rev. Lett. **72**, 172 (1994).

[12] T. Metcalfe, J.B. Knight, and H.M. Jaeger, Physica A **236**, 202 (1997); K.M. Aoki and T. Akiyama, Phys. Rev. Lett. **77**, 4166 (1996); E. Clément, L. Vanel, J. Rajchenbach, and J. Duran, Phys. Rev. E **53**, 2972 (1996).

[13] P.B. Umbanhowar, F. Melo, and H.L. Swinney, Nature (London) **382**, 793 (1996).

[14] J. Duran, J. Rajchenbach, and E. Clément, Phys. Rev. Lett. **70**, 2431 (1993); H.K. Pak, E. Van Doorn, and R.P. Behringer, *ibid.* **74**, 4643 (1995); L. Swinney, P. Umbanhowar, and F. Melo, in *Powders and Grains '93*, edited by C. Thornton (Balkema, Rotterdam, 1993), p. 369; F. Melo, P. Umbanhowar, and H.L. Swinney, Phys. Rev. Lett. **75**, 3838 (1995); H.K. Pak and R.P. Behringer, *ibid.* **71**, 1832 (1993); P. Evesque and J. Rajchenbach, *ibid.* **62**, 44 (1989); E. Clément,

J. Duran, and J. Rajchenbach, *ibid.* **69**, 1189 (1992); S. Fauve, S. Douady, and C. Laroche, J. Phys. (Paris), Colloq. **50**, C3-187 (1989); P. Evesque, Contemp. Phys. **33**, 245 (1992); O. Zik and J. Stavans, Europhys. Lett. **16**, 255 (1991).

[15] J. J. Moreau, in *Powders and Grains '93* (Ref. [14]), p.227.

[16] S. Luding, E. Clément, A. Blumen, J. Rajchenbach, and J. Duran, Phys. Rev. E **50**, R1762 (1994).

[17] G.C. Barker and A. Mehta, Phys. Rev. A **45**, 3435 (1992); Europhys. Lett. **27**, 501 (1994); Y-h. Taguchi, Int. J. Mod. Phys. B **7**, 1839 (1993); T. Pöschel and H.J. Herrmann, Europhys. Lett. **29**, 123 (1995); J.A.C. Gallas, H.J. Herrmann, and S. Sokołowski, J. Phys. II **2**, 1389 (1992); L. Rolf, Zem.-Kalk-Gips, **46**, 389 (1993).

[18] G.C. Barker and A. Mehta, Nature (London) **364**, 486 (1993).

[19] N.V. Brilliantov, F. Spahn, J.M. Hertzsch, and T. Pöschel, Phys. Rev. E **53**, 5382 (1996); see also G. Kuwabara and K. Kono, Jpn. J. Appl. Phys., Part 1 **26**, 1230 (1987); W.A.M. Morgado and I. Oppenheim, Phys. Rev. E **55**, 1940 (1997).

[20] Here we consider only the mode of external excitation ω_0. Since the higher frequencies ω_k are noncommensurable with ω_0 and with each other, the maximum acceleration of the superposition must be higher than $R(\omega_0)A_0\omega_0^2$. Hence consideration of higher modes will further increase the effect discussed here.